Neutral Atmospheric Effects on the Dissipation of Aircraft Vortex Wakes

A. J. Bilanin,* M. E. Teske,† and J. E. Hirsh‡
Aeronautical Research Associates of Princeton, Inc., Princeton, N.J.

Enhanced dispersion of two-dimensional trailed vortex pairs within simplified neutral atmospheric backgrounds is studied numerically for three conditions: when the pair is imbedded in a constant turbulent bath (constant dissipation); when the pair is subjected to a mean crosswind shear; and when the pair is near the ground. Turbulent transport is modeled using second-order closure turbulent transport theory. The computed results allow several general conclusions to be drawn with regard to the reduction in circulation of the vortex pair and the rolling moment induced on a following aircraft: 1) the rate of decay of a vortex pair increases with increasing background dissipation rate; 2) crosswind shear disperses the vortex whose vorticity is opposite to the background; and 3) the proximity of a ground plane reduces the hazard of the pair by scrubbing. The phenomenon of vortex bounce is explained in terms of secondary vorticity produced at the ground plane. Qualitative comparisons are made with available experimental data, and inferences of these results upon the persistence of aircraft trailing vortices are discussed.

Nomenclature

C = passive tracer ($C^* = C/C_0$)
C_ℓ = proportional to the induced rolling moment, Eq. (3)
q = root mean square of the turbulent kinetic energy, ($q^* = q2\pi s/\Gamma_0$)
r = radial coordinate measured from vortex center
s = initial semiseparation between vortices
t = time, $t^* = t\Gamma_0/2\pi s^2$
U_i = mean Cartesian velocity components
$\langle u_i u_j \rangle$ = ensemble-averaged Reynolds stress correlation
x_j = Cartesian coordinates
z_0 = hydrodynamic roughness length
β = normalized constant cross shear, $(2\pi s^2/\Gamma_0)\partial V/\partial z$
Γ_0 = initial circulation
ϵ = turbulent dissipation rate, $\epsilon^* = (2\pi)^3 s^4 \epsilon/\Gamma_0^3$
ζ = streamwise component of vorticity, $\zeta^* = \zeta 2\pi s^2/\Gamma_0$
Λ = turbulent macroscale parameter
ν = kinematic viscosity
σ = vortex spread parameter
ψ = streamfunction

I. Introduction

THE decay of aircraft vortex wakes has been the focus of extensive investigation by both NASA and DOT, in an effort to determine hazard potential and wake lifetime. Because of the inherent difficulty in making measurements in the wakes of aircraft, investigations have included the development of computer codes to simulate vortex behavior and predict vortex interaction. The work described herein are results from one such code "VORTEX WAKE."

Donaldson and Bilanin[1] present a review of the physics underlying vortex generation and decay, and the approaches used to analyze these effects. A comprehensive review of the entire subject has recently been given by Hallock and Eberle.[2] In Bilanin et al.[3] (hereafter referred to as "I"), we used the point-vortex approach of Rossow[4] to initiate a discussion of vortex merging, wherein vortices of like sign interact. The thrust in I was the application of turbulent transport theory to the merging process, to provide for a complete description of the convective and dissipative processes within the vortices themselves. The two-dimensional, unsteady numerical code "VORTEX WAKE" programs the Reynolds stress equations modeled by Donaldson.[5] The formulation of the modeled equation and the numerical procedures involved in solving them are included in I, as is an extensive discussion of the merging of multiple trailing vortices and the minimum hazard potential for a wing.

One important result from I is that a pair of opposite-signed vortices exhibit a surprisingly slow rate of decay when descending in a calm, neutral atmosphere away from the ground. These ideal conditions, fortunately, are not met often in practice. More commonly, vortex pairs encounter background turbulence, mean wind gradients, or the ground while descending in an atmosphere which is not in general neutrally stable. The effects of background turbulence, wind shear, and ground interaction form the subject of this paper. Here, we demonstrate through the use of our turbulent transport code that any of these quite naturally occurring effects may substantially reduce the lifetime of a vortex pair. Descent of a vortex pair in a stably stratified atmosphere will be the subject of a subsequent paper.

In Section II, we briefly review the turbulent transport model and examine a practical limit of the model used to provide idealized atmospheric environments. Improvements in the numerical code are also discussed here.

In Section III, we examine the effects of background turbulence on a vortex pair, showing that decay increases with increasing dissipation rate. In Section IV, we investigate the effects of mean shear and offer an explanation of the "solitary" vortex phenomenon. Finally, in Section V, we investigate vortex interaction with a ground plane and explain the phenomenon of vortex bounce which has been observed on runways and in subscale tests.

II. Turbulence Model and "VORTEX WAKE" Code

A need to predict turbulent transport in rapidly rotating, as well as stratified flows, led Donaldson to develop a second-order closure model of turbulent transport. A second-order model implies that partial differential equations are solved for the Reynolds stress tensor $\langle u_i u_j \rangle$ as well as for the mean ensemble-averaged U_i velocity components. Higher-order

Received Nov. 17, 1977; presented as Paper 78-110 at the AIAA 16th Aerospace Sciences Meeting, Huntsville, Ala., Jan. 16-18, 1978; revision received April 28, 1978.

Index categories: Boundary Layers and Convective Heat Transfer—Turbulent; Jets, Wakes, and Viscid-Inviscid Flow Interactions.

*Senior Consultant. Member AIAA.
†Consultant.
‡Associate Consultant.

unknowns and certain second-order correlations in the Reynolds stress equations are replaced by modeled terms containing constants and second-order correlations. These constants are evaluated by comparison with measurements made of fundamental fluid flows. A complete summary of the current state of incompressible modeling as used here may be found in Lewellen and Teske.[6] The following computations idealize the neutral atmosphere by assuming constant shear and homogeneous turbulence in the absence of a vortex wake. The background turbulence levels are determined by the "superequilibrium" limit of the turbulent transport model.[5] Superequilibrium limit is that turbulent fluid state which is approached at high Reynolds number when time rates of change and diffusion of second-order correlations are negligible.

When the diffusion and rate terms are set equal to zero in the rate equations for the second-order velocity correlations and a high Reynolds number is assumed, the resulting Reynolds stress equations for $\langle u_i u_j \rangle$ may be written as:

$$\overbrace{0 = -\langle u_i u_k \rangle \frac{\partial U_j}{\partial x_k} - \langle u_k u_j \rangle \frac{\partial U_i}{\partial x_k}}^{\text{production}}$$

$$\overbrace{-\frac{q}{\Lambda}\left(\langle u_i u_j \rangle - \delta_{ij}\frac{q^2}{3}\right)}^{\text{tendency towards isotropy}} \overbrace{-\frac{q^3}{12\Lambda}\delta_{ij}}^{\text{isotropic dissipation}} \tag{1}$$

where $q^2 = \langle u_i u_i \rangle$ and Λ is the turbulent macroscale. The production terms in Eq. (1) are balanced by a Rotta tendency-toward-isotropy term and an isotropic dissipation term. If the principle gradient is in the z-direction for the U velocity, for instance, then it may be shown that the solution to Eq. (1) is

$$q^2 = 2\left(\Lambda\frac{\partial U}{\partial z}\right)^2$$

$$\langle uu \rangle = \left(\Lambda\frac{\partial U}{\partial z}\right)^2$$

$$\langle vv \rangle = \langle ww \rangle = \frac{1}{2}\left(\Lambda\frac{\partial U}{\partial z}\right)^2$$

$$\langle uw \rangle = -\frac{\sqrt{2}}{4}\left(\Lambda\frac{\partial U}{\partial z}\right)^2$$

$$\langle uv \rangle = \langle vw \rangle = 0 \tag{2}$$

In the vicinity of a ground plane, the velocity gradient is inversely proportional to z (with z measured upwards from the ground), while the macroscale is proportional to z, maintaining a constant product of $\Lambda\partial U/\partial z$. Equations (2) are the boundary values for our turbulent correlations.

The mean and rate equations for the second-order correlations have been programmed into a two-dimensional unsteady incompressible computer code. The assumption of two-dimensionality implies that the phenomena to be investigated are such that axial gradients are insignificant and can be neglected. Therefore, sinusoidal instability and vortex breakdown are phenomena which cannot be addressed with this code.

The numerical solution technique (using an ADI scheme) is described in I. Several extensions to the code since the publication of I are the following. The mean equations have been reworked into streamfunction-vorticity variables, eliminating the need to compute the pressure. A direct solver developed by Swarztrauber and Sweet[7] determines the streamfunction, from which the velocity fields are obtained. In this way continuity is assured, even though a more difficult set of boundary conditions may sometimes result. To improve our simulation of the convective nature of the vortex flow problem, we now use a J_6 representation of the convective operator (Arakawa[8]), wherein the conservative and non-conservative operators are averaged.

For the specific computation of vortex pairs, an upwash velocity is added to keep the vortex pair in the computational domain. This is equivalent to sitting on the vortex pair as it descends. When the results are presented, however, the vertical coordinate is shifted to show the actual amount of descent. The choice as to what defines the position of a vortex is arbitrary. In I the centroid of the vorticity distribution was used to define vortex location. This definition was adequate for vortex pair computations in the absence of a ground plane. As will be shown later, however, when vortices interact with a ground plane, vorticity of the opposite sign is generated at the ground. This additional vorticity limits the usefulness of the centroid concept to fix position. To overcome this difficulty a passive tracer (neutral smoke) is initially prescribed in the center of the vortex and the location of the maximum of this passive tracer is taken as the vortex center. As the pairs spread by turbulent diffusion, readjustment of the numerical grid is undertaken to keep the boundaries away from the centers of vorticity. This readjustment does not cause any numerical problems.

As a convenience, initial distributions of vorticity, second-order turbulence quantities, and passive tracer are taken to be Gaussian. To reduce grid point requirements, whenever possible, half-plane computations are made. A uniform mesh is used except near the ground where additional resolution is, in general, needed to define the large shears that exist there.

III. Vortex Pairs in Constant Turbulent Backgrounds

In I the decay of a vortex pair in a constant dissipation rate turbulent bath was investigated to show that the dissipation rate itself was not sufficient to determine the rate of decay of vortices. It was shown that in a neutrally stable atmosphere, in the absence of mean crosswind shear, both the integral scale of the turbulent eddies Λ and the turbulent dissipation rate ϵ must be specified to fix vortex wake decay rate. In this section, additional computations are described and simple decay laws are deduced from the computations.

The computations were initialized by positioning a Gaussian of vorticity of the form $\zeta 2\pi s^2/\Gamma_0 = \pm(2/\sigma^2)\exp(-(r/s)^2/\sigma^2)$ at $y/s = \pm 1$, $z = 0$, respectively. The coordinate r is measured radially outward from the vortex center and σ is the vortex spread ($\sigma = 0.5$ for all computations). The numerical mesh is specified only for $y > 0$ since symmetries about $y = 0$ can be utilized. In addition to a uniform background level of turbulence, an isotropic Gaussian spot of turbulence is positioned in the center of each vortex of strength $(q_0 2\pi s/\Gamma_0)^2 = 0.01$, such that $\langle uu \rangle = \langle vv \rangle = \langle ww \rangle = (q_0^2/3)\exp[-(r/s)^2/\sigma^2]$. When a passive tracer is used, it begins with the same Gaussian character and has strength $C_0 = 1$. At the edges of the computation domain, except at the $y = 0$ boundary, turbulent quantities are assumed to reach the superequilibrium state and tracer concentration is set equal to zero. The streamfunction is obtained from moment expansion of the Biot-Savart law as described in I. The initial conditions are shown schematically in Fig. 1.

As a baseline computation the ambient turbulent field was set equal to zero and the decay of a vortex pair in a calm atmosphere was simulated. In this computation, as in all computations presented here unless otherwise noted, the integral scale parameter was initialized to be $\Lambda/s = 0.2$ and the Reynolds number was fixed at $\Gamma_0/\nu = 10^4$. The evolution of the scale is controlled by a dynamic scale equation detailed in I. As can be seen by examining the contour plots of vorticity for several times as shown in Fig. 2, a vortex pair in a calm atmosphere is predicted to dissipate very slowly. The vorticity

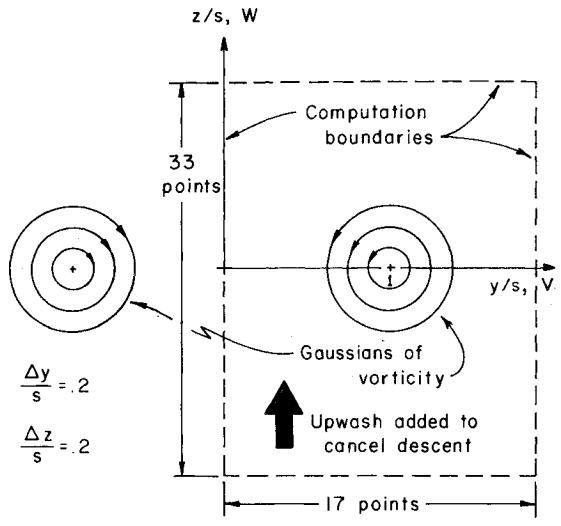

Fig. 1 Initial conditions for the computation of the decay of a vortex pair in a neutrally stable turbulent atmosphere.

distribution retains its shape initially (except for some slight vortex-on-vortex straining), and shows signs of trailing a wake after 20 vortex flow times. The vorticity level has dropped a factor of 10 below its initial value after 100 vortex flow times. For a typical landing B-747 aircraft, a flow time roughly corresponds to about 10 s. The apparent persistence of the vortex pair is not in agreement with observation.

A substantial increase in the decay rate occurs when the pair is placed in a turbulent flowfield. We assume that the turbulence is the result of a headwind gradient, $\partial U/\partial z$, such that the background turbulent level through Eq. (2) is nonzero and homogeneous.

If the scale length is taken to be $\Lambda/s=0.2$ and $(\partial U/\partial z)/(\Gamma_0/2\pi s^2)=0.56$ the dissipation rate, $(2\pi)^3 s^4\epsilon/\Gamma_0^3=0.0025$, is obtained. Isopleths of vorticity are shown in Fig. 3. In comparison with Fig. 2, it can be seen that substantial diffusion of the vorticity has occurred, with a drop in maximum value of an order-of-magnitude below the zero background case. In addition, the structure of the vortex pair has been noticeably altered. It is clear from the shape of the isopleths at times greater than $t\Gamma/2\pi s^2=20$ that the vortex pair leaves a wake of low-intensity vorticity. An extrapolation of the decay of the pair without background turbulence shows that over 10^4 flow times must pass before the zero background pair would decay to the same level as the decayed pair in 100 flow times.

Two quantities have been selected to quantify the amount of decay which occurs in a vortex pair; the circulation in a given area, and an integral which is approximately proportional to the rolling moment induced on a constant chord airfoil of semispan s_f. In Fig. 4 is shown the circulation computed about a square contour of dimension $2e\times 2e$ centered on the maximum of vorticity. The rate of decay as measured by Γ is independent of dissipation rate for sufficiently large times. These computations suggest that $\Gamma\sim t^{-2}$, which is expected from simple diffusion arguments that treat vorticity as passive tracer. Curiously, the $\epsilon=0$ computation has a long time decay of $\Gamma\sim t^{-1/2}$. This time behavior may be shown to be the diffusion limit of a turbulent decaying pair once mean fluid convection of vorticity is neglected. As a general expected observation, when the integral scale is initialized to be the same between turbulent atmospheres of comparable times after wake initialization, increased ϵ results in decreased circulation computed over a fixed contour. By far, however, it is our inability to quantify Λ in the atmosphere which precludes deriving a general decay curve for neutral turbulent atmospheres.

Corresponding rolling moment predictions for a follower aircraft having a coaxial encounter with the vortex are given in Fig. 5. Here the rolling moment is proportional to

$$C_l\alpha\int_{y_c-s_f}^{y_c+s_f} W(z_c,y)\,(y-y_c)\,dy \tag{3}$$

and y_c and z_c are chosen so as to maximize the integral at a given time. Typically, y_c and z_c are near the maximum in vorticity. The rolling moment curves for smaller follower aircraft are within 10% of the curves shown at these ϵ levels and are thus fairly represented by the $s_f/s=1$ curves. Again the rolling moment curve decays as $t^{-1/2}$ for the calm atmosphere and as t^{-2} for the turbulent atmosphere.

IV. Vortex Pair Subjected to a Cross-Flow Shear

Tombach[9] has observed during aircraft flight tests that under certain atmospheric conditions the smoke in one vortex would vanish while the second vortex remained intact. This phenomenon has come to be called the solitary vortex phenomenon. At the time of observation, it was conjectured that atmospheric shear might be responsible in some way. More recently, Rossow,[10] using distributions of point vortices, has shown that a vortex immersed in a cross shear is rapidly distorted when the shear is of opposite sign of the vorticity. Computations were undertaken to see if the large distortion in vortex structure could generate turbulence and thereby diffuse the smoke seeded in the vortex to make it visible.

The computation was initialized, as in Fig. 1, but now a cross shear of magnitude $\beta=(\partial V/\partial z)(2\pi s^2/\Gamma_0)=0.5$ was imposed. Figures 6a and 6b show isopleths of vorticity and turbulence. The vortex of sign opposite to the cross shear is distorted, which results in an increased turbulent level inside the vortex. Figure 6c is the computed dispersion of passive tracer which results. The fluid mechanisms in the enhanced dispersion of smoke in one vortex are now clear: it is the crosswind that is responsible for the phenomenon of the solitary vortex.

To quantify the decay of vortices in cross shear, the rolling moment was computed as shown in Fig. 7. Note that the rolling moment induced by the right vortex is about half that

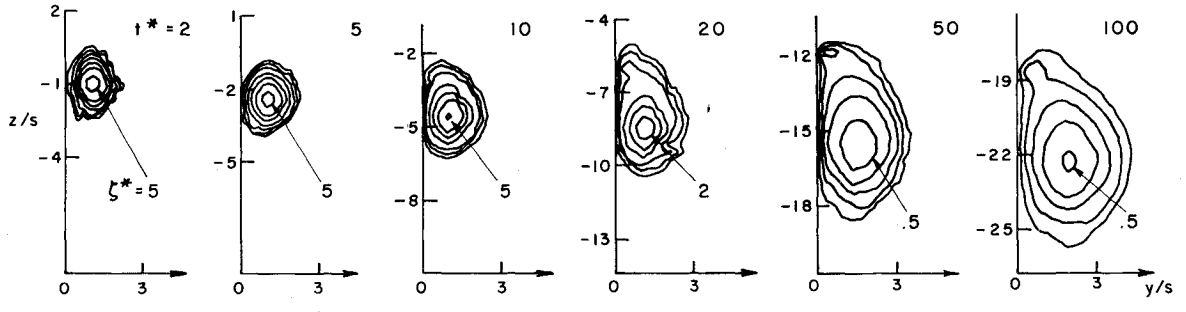

Fig. 2 Isopleths of vorticity for a vortex pair descending in a calm neutrally stable atmosphere. Maximum contour values are given with subsequent values taken from 5, 2, 1, 0.5, 0.2, 0.1, 0.05, 0.02, 0.01, 0.005.

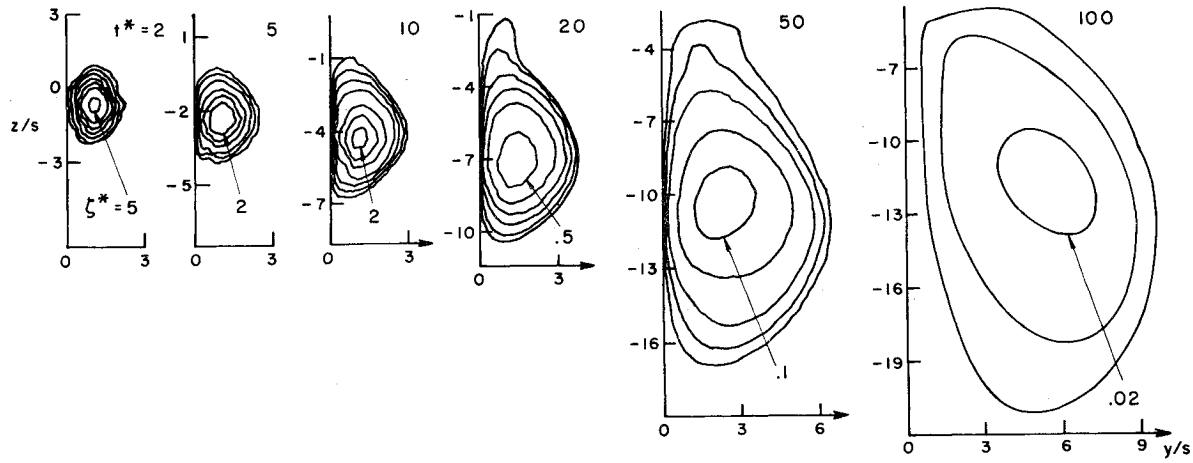

Fig. 3 Isopleths of vorticity for a vortex pair descending in a constant turbulent bath. Notation explained in Fig. 2.

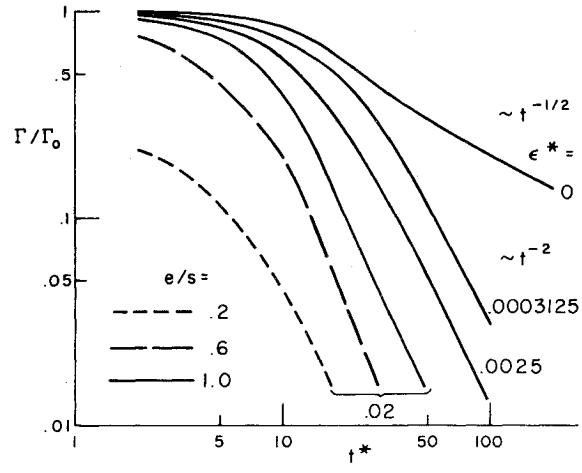

Fig. 4 Circulation dropoff as a function of time for square contours of size $2e \times 2e$ centered on the local maximum of vorticity for several background dissipation ratio $\epsilon^* = (2\pi)^3 s^4 \epsilon/\Gamma_0^3$.

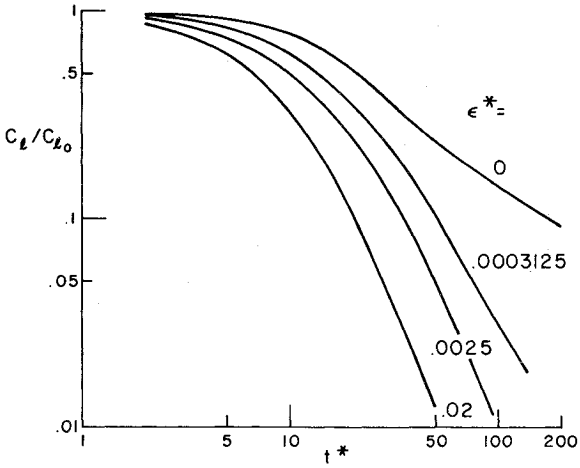

Fig. 5 Rolling moment dropoff as a function of time for a follower aircraft of semispan $s_f/s = 1$ having a coaxial vortex encounter within several background dissipation rates $\epsilon^* = (2\pi)^3 s^4 \epsilon/\Gamma_0^3$.

induced by the left vortex at six flow times. As can be seen at six flow times, both the right and left vortices induce rolling moments on a follower aircraft which are well below the rolling moments induced by the same vortex pair in a calm atmosphere. This general enhanced decay in the left vortex is attributed to the turbulent diffusion associated with the cross shear. It has been speculated that in the atmosphere over periods of tens of minutes it is possible to have shear without

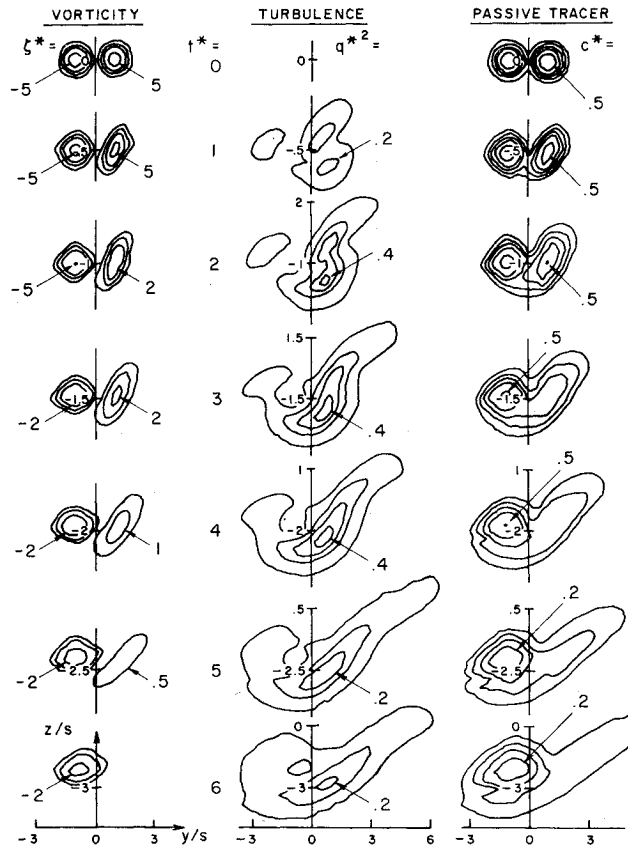

Fig. 6 a) Isopleths of vorticity of a vortex pair subjected to a cross shear. Values are ±5, ±2, ±1, ±0.5. b) Isopleths of turbulence for the pair in cross shear. Values are 0.4, 0.3, 0.2, 0.1. c) Isopleths of tracer for the pair in cross shear. Values are 0.5, 0.2, 0.1, 0.05, 0.02.

turbulence when the atmosphere is stably stratified. One might speculate that under these conditions the solitary vortex may indeed persist for long periods of time.

V. Vortex Pair in Ground Effect

One of the most perplexing observations of vortices has been the rebounding of a vortex as it approaches the ground. The phenomenon, we believe, was first observed by Dee and Nicholas[11] in 1968 and has been observed numerous times by researchers measuring vortex trajectories at airports.[12] In 1971 Harvey and Perry,[13] prompted by the above observation, conducted a series of tests in a wind tunnel with a moving floor to simulate correctly the ground plane. Using total head probes they concluded that the proximity of the vortex to the ground plane could result in boundary-layer

separation and secondary vorticity which could explain the upward migration of the vortex pair.

The computer code was modified to include a viscous ground plane in an effort to simulate the ground interaction. The surface is fixed at a level plane $z=z_0$ (where z_0 is the roughness height). As far as the streamfunction boundary conditions are concerned, this surface is merely another reflecting plane across which opposite signed image vortices influence the flow (much as the image vortex of strength $-\Gamma_0$ did in Secs. III and IV). The vortex pair is assumed sufficiently close to the surface so that the velocity gradient

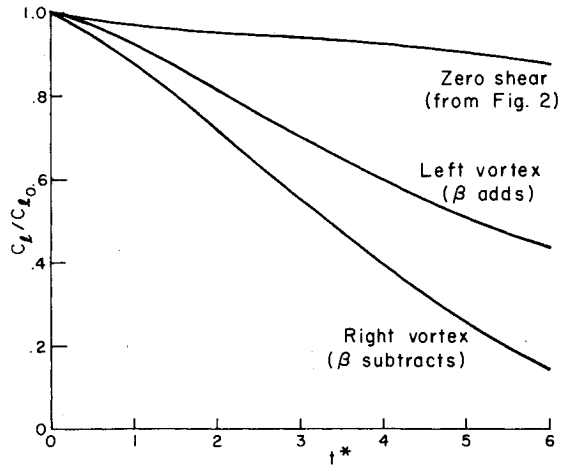

Fig. 7 Rolling moment dropoff as a function of time for a follower aircraft of semispan $s_f/s=1$ having a coaxial encounter. Normalized constant cross shear is $\beta=0.5$.

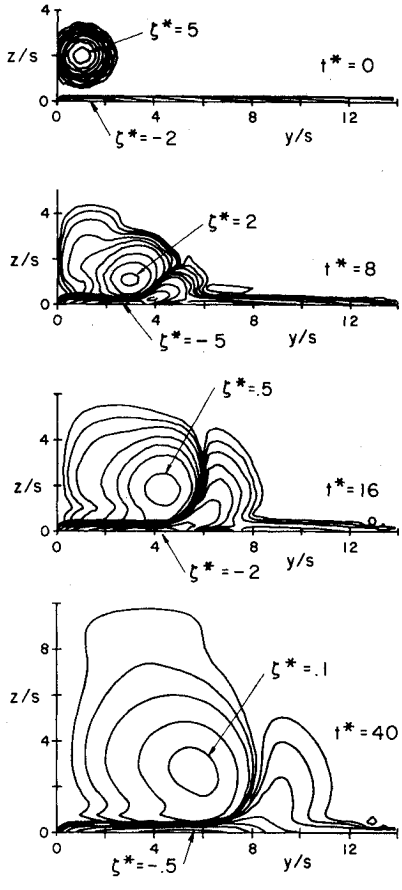

Fig. 8 Isopleths of vorticity for a vortex pair descending toward a ground plane. Positive contours around the vortex follow from the given maximum values as given in Fig. 2. Negative contours generated near the wall follow −5, −2, −1, −0.05, −0.02, −0.01, −0.005.

$\partial U/\partial z$, maintaining a small turbulence level, may be taken to be inversely proportional to z. Since the scale length is proportional to z in the Monin-Obukhov sublayer, the background turbulence level may still be taken as constant. All necessary turbulence quantities, however, will be given zero vertical gradients at the hydrodynamic roughness height. We relate the vorticity level at the surface to the streamfunction there by a finite difference representation of the Poisson equation and the velocity law-of-the-wall to give:

$$\eta_r = -\frac{2(\psi_+ - \psi_r)}{(\Delta z)^2\left[1+\dfrac{2z_r \ell n(z_r/z_0)}{\Delta z}\right]} \tag{4}$$

where ψ_+ is the streamfunction value at $z_+ = z_r + \Delta z$, and z_r is the reference z height above z_0 (typically $z_r/s=0.01$). When the flow simulation begins, Eq. (4) gives an immediate surface vorticity layer of opposite sign to the vortex convecting toward the surface from above. A sequence of contour plots of vorticity for the case where $z_0/s=10^{-4}$, with the vortices initially positioned at $y/s=\pm 1$, $z/s=2$, is shown in Fig. 8.

As the vortex approaches the ground (its mate is across the reflecting plane at $y=0$), the boundary layer beneath grows and separates, resulting in a secondary vortex. The secondary vortex is of the opposite sign to the descending vortex around which it is advected. The secondary vortex induces an upward and outward motion on the descending vortex pair, which results in a rebound (bounce) of the pair away from the ground plane. The rebound phenomenon described here suggests that the classical "inviscid" description of a pair of vortices following a hyperbolic trajectory may not be a particularly good model. Figure 9 shows the computed trajectories of the maximum values of passive tracer. Note that a laminar computation undertaken at $\Gamma_0/\nu=100$ also permits the rebounding phenomenon to occur.

Curiously, Barker and Crow[14] have recently investigated vortex pairs in ground effect and have attributed the rebound to effects of finite vortex core radius. To demonstrate that this explanation is suspect, we performed a computation with an inviscid boundary condition applied on the ground (vanishing of vertical velocity). The vortex spread, $\sigma=0.5$, is used and the results of the computation are also summarized in Fig. 9. As can be seen, the rebounding phenomenon does not occur unless the viscous boundary condition is applied, even though the vortex cores are of finite size. It is seen that the finite difference solution with inviscid ground plane is in good agreement with the hyperbolic point vortex trajectories. The slight drift upward results from diffusion of the smoke.

The decay which results from scrubbing along a viscous ground is presented in Fig. 10. Included is the rolling moment decay curve with zero background turbulence taken from Fig. 5. As can be seen, interaction with the ground provides a mechanism which greatly reduces the rolling moment induced on a follower aircraft over that induced by the same vortex pair left to decay out of ground effect.

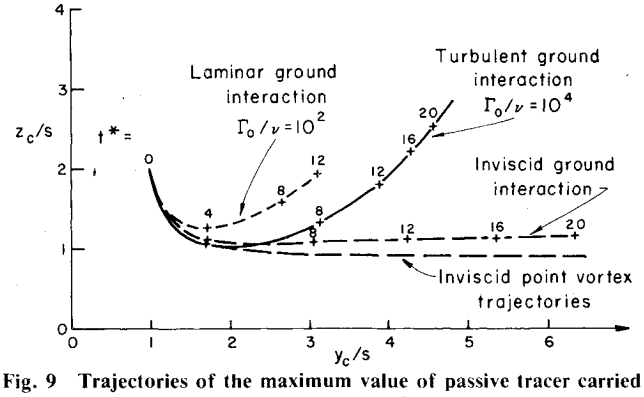

Fig. 9 Trajectories of the maximum value of passive tracer carried by a vortex pair descending onto a ground plane.

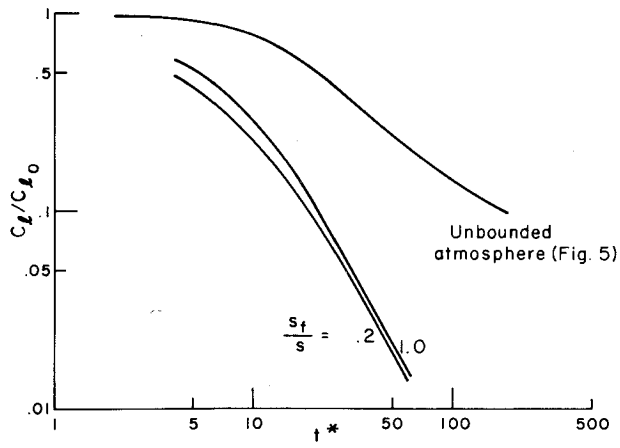

Fig. 10 Rolling moment dropoff as a function of time for follower aircraft having coaxial encounters with a vortex interacting with the ground.

VI. Conclusions

Two-dimensional aircraft trailing vortex pairs descending in a neutral atmosphere are shown to have enhanced dispersion when the atmosphere is turbulent, when crosswind shears are present, and when the vortices interact with the ground. These results are predictions from the finite difference computer code, "VORTEX WAKE," which uses second-order closure turbulent modeling to include turbulent transport. In particular, the following conclusions are drawn with regard to neutral atmospheres:

1) The decay of a vortex pair immersed in a turbulent bath is enhanced with increasing dissipation rate, providing the integral scale of the turbulence remains constant. In general, however, the dissipation rate, even in neutral atmospheres, is insufficient to quantify dispersing effectiveness of the atmosphere.

2) The phenomenon of the solitary vortex is shown to result as a consequence of crosswind shear. The vortex having the sign of vorticity opposite that of the vorticity in the shear is convectively distorted, producing turbulence in the vortex. This turbulence then disperses the smoke which was introduced in the vortex for visualization purposes.

3) The classic inviscid notion that a vortex pair descending towards a ground plane follows a trajectory that is hyperbolic is generally not correct. The vortex pair rebounds or bounces away from the ground as a result of separation of the ground boundary layer below the vortex. It is shown that this separation results in secondary vortices which induce a velocity on the descending vortices outward and upward, thereby explaining the rebounding phenomenon. It is speculated that when crosswinds are present symmetries of the secondary vortices are destroyed. This could result in the observed tipping of the descending pair.

Acknowledgment

This work was sponsored by NASA Langley Research Center under Contract NAS1-14707.

References

[1] Donaldson, C. duP. and Bilanin, A. J., "Vortex Wakes of Conventional Aircraft," AGARDograph 204, May 1975.

[2] Hallock, J. N. and Eberle, W. R., "Aircraft Wake Vortices: A State-of-the-Art Review of the United States R&D Program," FAA Rept. FAA-RD-77-23, Feb. 1977.

[3] Bilanin, A. J., Teske, M. E., and Williamson, G. G., "Vortex Interactions and Decay in Aircraft Wakes," *AIAA Journal*, Vol. 15, Feb. 1977, pp. 250-260.

[4] Rossow, V. J., "Inviscid Modeling of Aircraft Trailing Vortices," *Proceedings of the NASA Symposium on Wake Vortex Minimization*, Washington, D.C., Feb. 25-26, 1976, pp. 4-54.

[5] Donaldson, C. duP., "Atmospheric Turbulence and the Dispersal of Atmospheric Pollutants," *AMS Workshop on Micrometeorology*, edited by D. A. Haugen, Science Press, Pa., pp. 313-390.

[6] Lewellen, W. S. and Teske, M. E., "Turbulence Modeling and Its Application to Atmospheric Diffusion," EPA-600/4-75-016, 1975.

[7] Swarztrauber, P. and Sweet, R., "Efficient Fortran Subprograms for the Solution of Elliptic Partial Differential Equations," NCAR-TN/IA-109, July 1975.

[8] Arakawa, A., "Numerical Simulation of Large-Scale Atmospheric Motions," in "Numerical Solution of Field Problems in Continuum Physics," *SIAM-AMS Proceedings*, Vol. 2, 1970, pp. 24-40.

[9] Tombach, I., "Observations of Atmospheric Effects of Vortex Wake Behavior," *Journal of Aircraft*, Vol. 10, Nov. 1973, pp. 641-647.

[10] Rossow, V. J., "Convective Merging of Vortex Cores in Lift-Generated Wakes," AIAA Paper 76-415, San Diego, Calif., July 14-16, 1976.

[11] Dee, F. W. and Nicholas, O. P., "Flight Measurements of Wing Tip Vortex Motion Near the Ground," CP1065, British Aeronautical Research Council, London, 1968.

[12] Bradshears, M. R., Logan, N. A., and Hallock, J. N., "Effect of Wind Shear and Ground Plane on Aircraft Wake Vortices," *Journal of Aircraft*, Vol. 12, Oct. 1975, pp. 830-833.

[13] Harvey, J. K. and Perry, F. J., "Flowfield Produced by Trailing Vortices in the Vicinity of the Ground," *AIAA Journal*, Vol. 9, Aug. 1971, pp. 1659-1660.

[14] Barker, S. J. and Crow, S. C., "The Motion of Two-Dimensional Vortex Pairs in a Ground Effect," *Journal of Fluid Mechanics*, Vol. 82, Pt. 4, 1977, pp. 659-671.